J Therm Anal Calorim (2010) 102:671–680
DOI 10.1007/s10973-009-0613-3

Metastable effects on martensitic transformation in SMA

Part VIII. Temperature effects on cycling

V. Torra · C. Auguet · A. Isalgue · F. C. Lovey · A. Sepulveda · H. Soul

Received: 17 October 2009 / Accepted: 17 November 2009 / Published online: 10 December 2009

Abstract The use of Shape Memory Alloys (SMA) in technical applications as damping in civil engineering structures requires the characterization of the alloy for each specific application. This involves the evolution of the mechanical properties and damping capacity with the number of cycles, frequency, maximum deformation, applied stresses, and the evolution of the alloy with aging time and temperature. In particular, the temperature effects associated to self-heating need to be evaluated. In continuous cycling the effects of latent heat, the associated dissipation induced by the hysteresis, the heat flow to surroundings and the cycling frequency induce different states of temperature in the specimen, which in turn produces changes in the transformation-retransformation stresses. In this article, the temperature effects associated to cycling are outlined for different cycling frequencies. The results show that, for relatively faster frequency the temperature arrives at an oscillatory state superimposed to an exponential increase. For lower frequencies, some parts of the sample attain temperatures below room temperature. The experimental results are represented with an elementary model (the 1-body model or the Tian equation used in calorimetric representation) of heat transfer. For the higher fracture where life requirements are associated to damping in stayed cables for bridges, the results show (for the NiTi alloy) a reduction of the hysteresis width as the frequency increases for deformations up to 8%. For reduced deformation, under 2% appears an asymptotic behavior where the frictional area is practically independent of the cycling frequency (up to 20 Hz). In addition, it is shown that more than 4 million of working cycles can be attained if the maximum applied stress is kept below a threshold of about 200 MPa. Although under this condition the deformation must remain lower than 2% a reasonable damping capacity can still be obtained.

Keywords Shape memory alloys · Phase transformation · Latent heat · Hysteresis cycle · Damping · Passive systems · Self-heating · Damping of stayed cables

V. Torra (✉) · C. Auguet · A. Isalgue
CIRG, DFA, ETSECCPB, UPC, Campus Nord B4,
08034 Barcelona, Catalonia, Spain
e-mail: vtorra@fa.upc.edu

A. Sepulveda
Facultad de Ciencias Físicas y Matemáticas, Universidad de Chile, Beauchef 850, Santiago 8370448, RM, Chile
e-mail: asepulve@cec.uchile.cl

F. C. Lovey · H. Soul
Centro Atómico Bariloche and Instituto Balseiro, 8400, San Carlos de Bariloche, Argentina

F. C. Lovey
e-mail: lovey@cab.cnea.gov.ar

Introduction

Recently, the SMA's were proposed as useful passive devices for dampers in Civil Engineering [see 1 and related references]. The SMA produces hysteresis in their martensitic transformation (a called first order phase transformation of "military" characteristics). In the stress-induced transformation (parent to martensite), a heat ($Q_{p\to m}$) is released corresponding to the macroscopic effect of the latent heat per volume unit $\ell(\sigma_{tr})_{p\to m}$, which is a function of the applied stress to transform, σ_{tr}, and in reverse action (martensite to parent) the heat ($Q_{m\to p}$) related to the latent heat $\ell(\sigma_{ret})_{m\to p}$ is absorbed by the alloy, where σ_{ret} is the re-transformation stress.

In general, σ_{tr} and σ_{ret} are not constant but depends on the amount of transformed material. In a close cycle involving the forward and backward process without intrinsic changes or change of internal energy (i.e., without creation of dislocations or changes in atomic order), the Hysteretic Work (HW) corresponding to the mechanical work dissipated as heat is related by the First Law to absorbed and released heats by:

$$HW = \oint \vec{f}\, d\vec{x} = Q_{p \to m} + Q_{m \to p} \tag{1}$$

The balance equation (1) is only valid when the shape of the hysteresis cycle remains strictly invariant. For each application an appropriate guaranteed behavior of the main material parameters are required. For instance, a macroscopic or mesoscopic property as the hysteresis cycle requires a well determined study of its evolution in cycling. For instance, the effects of the cycling frequency, of the maximum deformation, of the applied stress and also, of the evolution of aging time and temperature need to be carefully analyzed. In addition, the temperature effects associated to self-heating need to be evaluated (part 3). In continuous cycling, the effects of latent heat and the dissipation due to the hysteresis produces local changes in the specimen temperature. This is also related to the heat flow to/from the surroundings and with the cycling frequency. Also, that the spontaneous increase of length of the sample with cycling: (the SMA creep) has to remain under control ensuring effective damping with the expected length.

The damping effect relates the absorption of mechanical work HW and its transformation as heat in the sample to be dissipated in the surroundings. In general, the self-heating is intrinsic to damping equipments and needs to be analyzed to avoid temperature increases and eventual damage of devices. Since the dissipated and absorbed heat takes place at different stresses, a thermodynamic description of the hysteretic cycle establishes that the latent heat is different in transformation that in retransformation by the HW value that is fully converted in heat.

In the previous articles of these series, several thermal and thermomechanical properties were studied. These properties are of the major importance for the applications of CuAlBe and NiTi Shape Memory Alloys in particular damping devices. See, for instance, the articles entitled "Metastable effects on martensitic transformation in SMA" (Parts 1–7) [2–8]. The applicability in dampers of stayed cables requires several millions of working cycles without fracture of SMA at "higher frequencies" (higher than 1 Hz). In the Iroise Bridge, the main observed frequencies are 1 and 3 Hz and also, 18 Hz in the St Nazaire Bridge.

In this article, the study is focused in self-heating and in the availability of the faster cycles for damping. An elementary model of heat transfer describes the macroscopic behavior of the temperature on the damper showing that the temperature effects are decisive in the hysteretic behavior for NiTi wires. Partial analysis is devoted to the experimental results associated with low deformation cycling ensuring higher fracture-life. Low deformation, in order to get a maximum applied stress of about 200 MPa, is required to ensure great number of working cycles (several millions) and it is also compulsory to determine the self-heating effects and the hysteretic effects at "higher" cycling frequencies related with the stayed cables in bridges.

Experimental

Several sets of measurements of stress–strain are carried out using a MTS 810 with a Hydraulic Power Unit (MTS silent flow 505.11). A roughly approach to the sample temperature is obtained using one K thermo-pair of chromel–alumel (furnished by OMEGA) with thinner wires mechanically connected to the samples. In particular using a DMM Agilent model U1251A that via a proprietary program permits 6.4 reading/s.

Three types of samples were used all in polycrystalline state: CuZnAl prepared at an university laboratory, in an induction furnace, from ingots of copper (Electrolytic Tough Pitch, C11000, 99.9 wt% purity), aluminum (Aluminium Association 1050, 99.5 wt% purity) and zinc (Special High Grade, 99.99 wt% purity), CuAlBe, and NiTi. The composition on the first alloy determined by Optical Emission Spectroscopy (OES) is Zn: 17.04 wt%, Al: 7.24 wt%, Ms: 278.1 K, Af: 295.2 K measured by DSC. For the CuAlBe, the cast AH140, the nominal values determined by Trefimetaux are: Ms = 255 K; Mf = 226 K; As = 253 K; Af = 275 K, with composition Al = 11.8 wt%; Be = 0.5 wt%; Cu = balance. The composition for the NiTi alloys, (furnished by SAES Getter) is Ni = 55.90 wt%, Ti = balance with some other parasitic elements in the ppm range (C: 267 ppm, O: 269 ppm).

The CuAlZn and CuAlBe requires some thermomechanical treatment ensuring that the samples are, effectively, in the parent phase. For the CuAlZn, the sample is homogenized and later quenched in water at room temperature. For the established heat treatment in CuAlBe see the references [3, 4]. Furthermore, some short homogenization processes (10, 20, and 30 min at 820°C) are studied to ensure appropriated fatigue-life for the applications (damping of earthquakes) when samples with higher lengths were required (i.e., 70 or 80 cm).

Self-heating in cycling

Figure 1 shows the self-heating effect related to latent heat and hysteretic behavior for CuAlZn alloy for series of stress–strain cycles at 323 K and 3% of deformation. Using a sampling of 1 s, the digitizer permits a reasonably evaluation of temperature behavior for cycling frequency near to 0.1 Hz.

The mean temperature shows an oscillatory behavior partially around the mean (room) temperature as expected because of the heat loses to surroundings (see below the part 4).

Avoiding changes in the hysteretic behavior, the dissipated power due to the hysteresis (heating) is proportional to the cycling frequency and the heat loses by natural or forced convection is reduced with the length in time of the cycles. At lower frequency (0.1 Hz), the temperature shows a temperature wave with negative part (temperature under the room temperature). The negative part progressively disappears when the frequency increases. The effect is roughly outlined in Fig. 1 or in Fig. 2 (CuAlBe alloy) for cycling frequency of 0.1, 0.5, and 1 Hz.

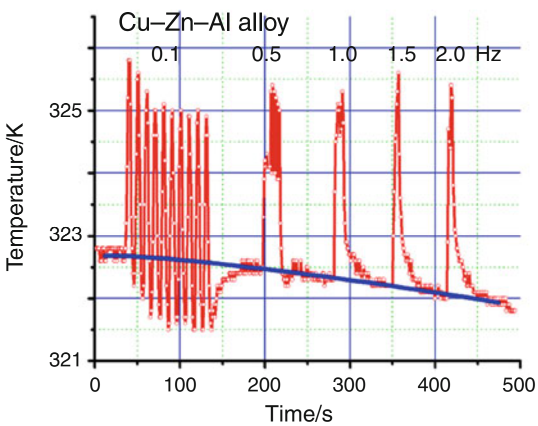

Fig. 1 Temperature effects on stress–strain cycling in CuAlZn, using temperature sampling of 1 Hz (one data/s). The "base line" indicates that the "room temperature" (323 K) is spontaneously reduced by roughly 1 K

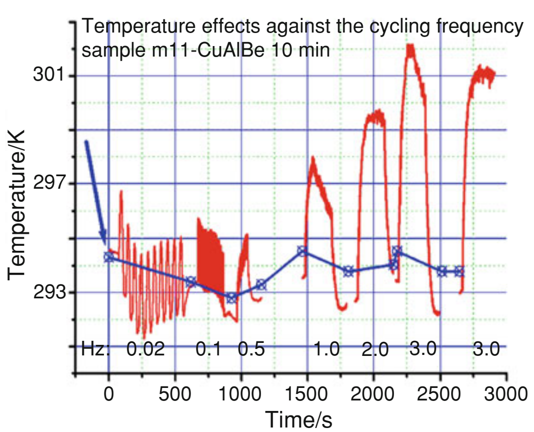

Fig. 2 Temperature effects in a CuAlBe alloy, evolution of the sample temperature with the cycling frequency for one maximal deformation of 8%. The *arrow* indicates the dots and line that show a rough representation of the room temperature time evolution (near 2 K peak to peak, with faster fluctuations)

The effect relates the heating–cooling by the transformation and also, the cooling to surroundings by spontaneous or forced convection. When the sample starts to re-transform the temperature associated to latent heat is reduced by the spontaneous cooling and the absorption of latent heat in retransformation reduces the temperature under the room temperature. A second set of data, relates cycles on the CuAlBe alloy up to 3.14% of deformation (previously homogenized by 10 min at 1,093 K) for a series of progressive increased frequencies as shows the Fig. 2. The results are similar to those from CuAlZn but in this case the mean digitizing sampling is 0.1554 s or 6.4 reading/s. The DMM only furnishes, for higher cycling freq, the temperature changes are relatively reduced in comparison with fluctuations of room temperature. The temperature in Fig. 2 shows the effects of room temperature fluctuations (2 K peak to peak) partially induced by the on–off actions of the conditioning air device. The mean net increase of temperature is relatively small (i.e., less than 10 K), consequently the associated stress effects for CuAlBe do not overcome 20 MPa [5].

The study of NiTi is performed at several levels of approach. First, the temperature effects and the associate time scales are evaluated for a thinner wire (0.5 mm of diameter, 101 cm of total length) using a home-made stress–strain-temperature device. Figure 3 shows the hysteresis cycle when is described using series of steps in

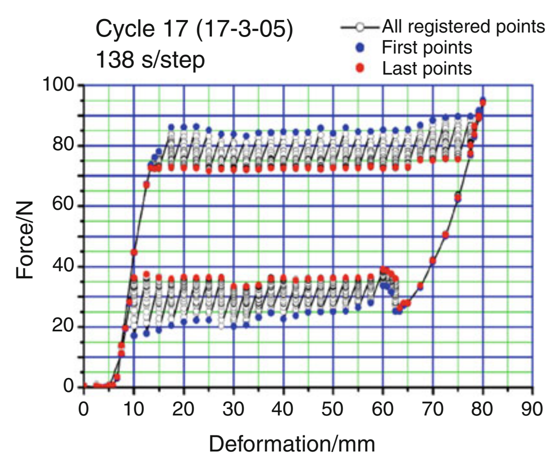

Fig. 3 Temperature effects on the hysteretic behavior in a NiTi sample of 1.01 m and 0.5 mm of diameter. The external data relate the instantaneous force after an elementary step in length (2.5 mm) and the inner data correspond to measured force after 138 s

deformation (each step produces a length change of 2.5 mm). Each fast deformation step induces a step in force (stress) against the time in transformation or in retransformation produced by the released or absorbed latent heat. The effect of fast step plus one larger pause permits the visualization of local temperature increase via their force action (Clausius–Clapeyron coefficient or d*f*/d*T*). After each load step the material shows a transitory behavior approaching the thermal equilibrium (Fig. 4). After 138 s of the step, the force reduces from 84 to 72 N (a change of 61 MPa) in transformation and similar value in retransformation (see Figs. 3, 4). The mean difference in the hysteretic width (Fig. 3) approaches from 341 to 188 MPa from fast to slow reading. The mean reduction of hysteresis indicates the relevance of thermal effects and that an isolated value of the hysteresis width is, usually, an ill defined parameter, highly dependent of the cycling frequency and used material.

The required time for one complete cycle (i.e., represented in Fig. 3) is close to 3 h (roughly a cycling mean frequency of 0.0001 Hz). Figure 4 (left and right) outlines the evolution of the force with time after each displacement step in loading or in unloading. The measurement is realized by 31 complete steps of 2.5 mm of displacement plus 6 steps of 1/3 of displacement. The 1/3 step are used for satisfactory resolution when the branch of the cycle are stepped. The retransformation is realized via 28 complete steps plus 15 steps of 1/3. The force sensor (HBM type U9B/20kN) with amplifier MVD2510 associate to a digitizer: DMM Keithley 2000. The use of a GPIB-bus with an appropriate proprietary program permits a series of readings showing a progressive decrease (increase) of the stress in transformation (retransformation). Figure 3 shows the general overview of the measurement.

The force steps are separated by 138 s (in transformation or retransformation; Fig. 3 or 4) that roughly represents 12 N or 61 MPa. The Clausius–Clapeyron equation establishes that the stress change represents a local change of temperature close to 9 K: an increase in transformation and a decrease in retransformation. The global effect of force versus temperature steps was a change of local hysteresis width. Really, the hysteresis cycle is highly dependent of the cycling frequency, the natural or forced convection and of the sample diameter.

The observed results for NiTi of 0.5 mm of diameter shows that some change of behavior can appear between "lower" and "higher" cycling frequencies (for instance, between 0.0001 and 1 Hz or for higher frequencies). In transformation, the temperature increases due to the release of latent heat in transformation creating a "warmed wave". At relatively low cycling frequencies the advancement of transformation front occurs inside the local heated front. Therefore, some supplementary stress (as shows the Fig. 4 left) is needed to proceed with the transformation. In fast cycling the advancing transformation front remains ahead of the temperature front, thus lower stress is required to transform. For instance, only the stress associated to the mean temperature of the sample is required.

Heat diffusion and transformation front

The heat diffusion indicates that a heat pulse is progressively broadened and expanded with a displacement x in the time t in a Gaussian shape by a thermal diffusion coefficient D, via:

$$x^2 = 2Dt \tag{2}$$

A rough approach to the speed of temperature front propagation reads,

$$v_T = \frac{\Delta x}{\Delta t} = \sqrt{\frac{2D}{\Delta t}} \tag{3}$$

The mechanical approach to the front propagation, for a complete transformation, i.e., 8% of deformation for a sample with 200 mm length, suggests that the value of its speed (v_M) approaches:

$$v_M = l_u/\Delta t \tag{4}$$

The l_u is the free sample length (for instance between the grips) and the Δt is the time necessary to complete a half of the cycle:

$$\Delta t = 1/(2f) \tag{5}$$

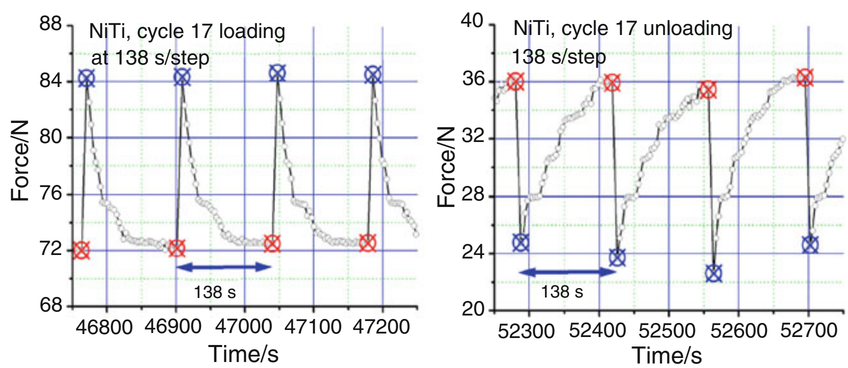

Fig. 4 Force evolution after one displacement step. *Left*: effects of loading (parent to martensite). *Right*: effects in unloading (martensite to parent)

Table 1 Values of v_M and v_T for different values of the cycling frequency

f/Hz	0.0001	0.001	0.01	1
v_M/mm s^{-1}	0.02	0.2	2	200
v_T/mm s^{-1}	0.04	0.13	0.4	4

The value for the thermal diffusion coefficient in NiTi ($D = 4.02\ 10^{-6}$ m^2 s^{-1}) is extracted from [9]

The definition of v_M is a crude approach. Usually the cycles are performed using sinusoidal deformation program and the value of v_M is continuously changed from maximal value to zero. The f value is the cycling frequency. The crude approach outlined indicates a difference of behavior between the "thermal speed" and the "mechanical speed". For instance, the speed values are reversed for cycling frequencies near 0.001 Hz (see Table 1). The experimental measurements suggest that the reversion of v_M and v_T is close to 0.01 Hz.

The just mentioned rough approach to front propagation speed suggests that at lower cycling frequencies the mechanical front remains inside that the thermal wave. In transformation/retransformation, the required stress is higher/lower than necessary when the material is at the mean room temperature. At higher frequencies the action is reversed, the thermal front tracks the mechanical front with a progressive delay as the cycling frequency increases. The new transformation zone is in contact only with the mean temperature arising from the mean previous hysteretic dissipation with a weak effect of the actual transformation front.

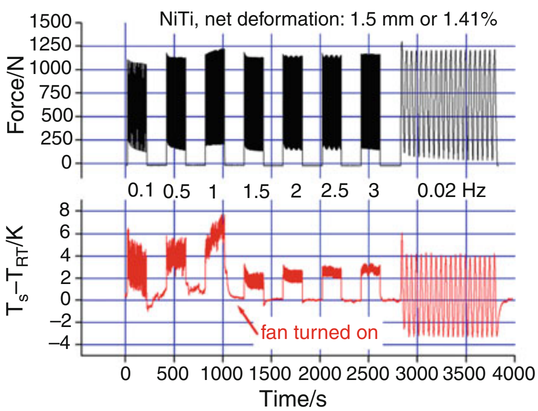

Fig. 5 NiTi SMA, force, and excess temperature against time for several cycling frequencies at lower deformation (near 1.5%). The activation of a fan at $t = 1{,}000$ s, reduces the excess temperature to a half and the force also changes accordingly the Clausius–Clapeyron equation (6.3 MPa/K) and the wire diameter (2.48 mm)

Cycling frequency effects on damping capacity

The studies for CuAlBe and NiTi alloys using sampling of 0.154 s permit a reasonable sampling and display of cycles up to 1 Hz (see Figs. 2, 5, 6). Later, for cycling frequencies near or over 2 Hz the sampling is insufficient and only some "mean temperature value" can be obtained.

Series of tests are carried out in NiTi alloy, basically for two deformations {complete transformation (8%) and lower partial transformation: less than 2%}. The temperature effects determined in one point of the sample (near the center) by a K type thermocouple (wire of 0.1 mm of diameter) are clearly related with the air cooling effect from the external air movement. Figure 5 clearly shows the action of a fan. The increase of "wind" on the sample (from natural convection to forced convection) reduces the temperature span to a half (as shows the Fig. 5). At lower cycling frequency 0.1 Hz in Fig. 1 and 0.02 Hz in Fig. 2, the temperature "tracks" the external force with a temperature wave over and under the room temperature (Fig. 6), respectively.

For 0.01 Hz the temperature is practically "symmetrical" (see, Fig. 6), for 0.1 Hz, the heating related to the hysteresis cycle is progressively more relevant, and for frequencies greater than 0.1 Hz, (deformation 8%) the temperature remains higher than room temperature (see, for instance, the Fig. 6 left; 0.01 Hz) and the cycling studies at 0.05, 0.5, 1, 2, and 3 (A–B–C–D, and E) in Fig. 6 (right). However, the effect is not relevant for lower deformation

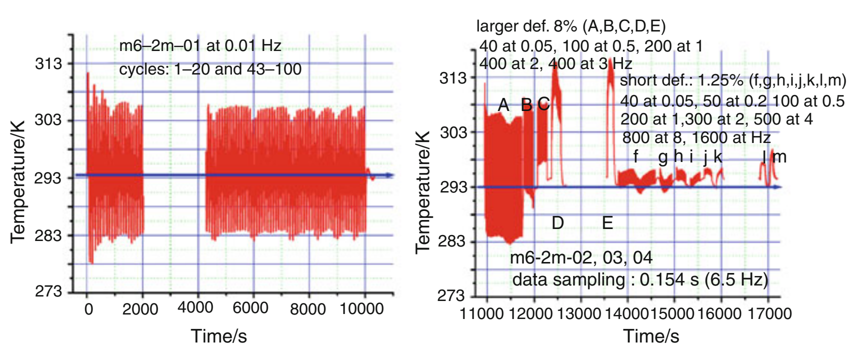

Fig. 6 Temperature effects in NiTi alloy with a progressive increase of the cycling frequency. *Left*: cycling frequency 0.01 Hz. The room temperature is close to 20 °C. *Right*: sets of measurements: A–B–C–D–E with 8% of deformation, and f–g–h–i–j–k–l–m with 1.25% of deformation. The temperature sampling approaches 6.5 reading/s

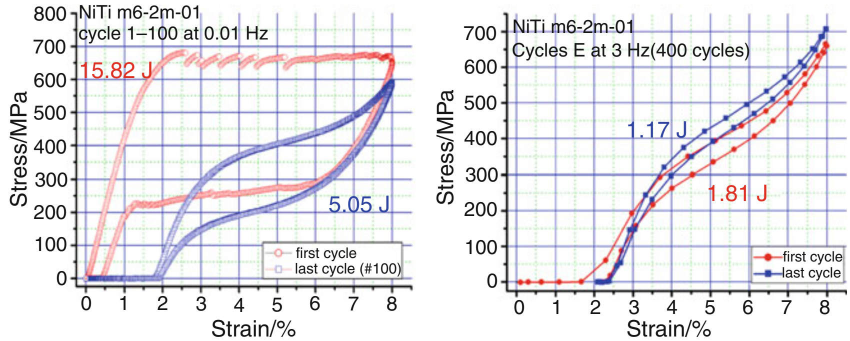

Fig. 7 First and last cycle of each set of cycles. *Left*: evolution of the first 100 cycles at 0.01 Hz with 8% of maximal deformation. *Right*: evolution of 400 cycles at 3 Hz with the 8% of maximal deformation

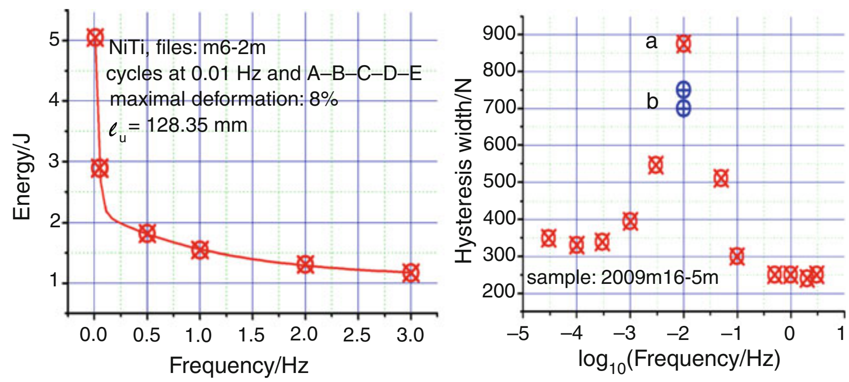

Fig. 8 NiTi: cycling frequency effects on the hysteretic behavior for 8% deformation (*dots*). *Left*: Changes in hysteretic energy for the sets of cycles A–B–C–D–E in Fig. 6 *right*. *Right*: Evolution of the hysteresis width against the cycling frequency

(<2%), see the sets of measurements at 0.05, 0.2, 0.5, 1, 2, 3, 4, 8, and 16 Hz (f, g, h, i, j, k, l, and m). For instance, under the fan action, the mean temperature increase does not overcome 8 K for cycling frequencies as "faster" as cycling at 16 Hz.

The information obtained for temperature data depends on the sampling frequency and amount of deformation. The analysis is limited to near 0.2 Hz when the sampling is 1 s (Fig. 1). The sampling at 0.154 s is used in Figs. 2, 3, 5, and 6. From the point of view of the mean temperature effects, the Fig. 6 suggests that the NiTi can work for relatively faster cycling frequencies when lower deformation is used. In fact, the temperature increase seems roughly proportional to the percent of deformation. From the sets of cycles D–E to sets f–g the temperature is roughly divided by 8. Increasing the cycling frequency with a maximal deformation of 8% the hysteresis cycle is progressively modified and the hysteretic energy is, also, progressively reduced (see, Fig. 7 left and right). The main mean effect on the hysteretic energy against the cycling frequency was represented in the Fig. 8.

At 8% deformation, the dissipated energy decays from 15.82 to a 5.05 J in the training process (100 cycles at 0.01 Hz). After, the dissipated energy can attain a minimum 1.17 J when cycled at frequencies near to 3 Hz. The reduction of the hysteresis width during the training procedure is most probably due to the creation of dislocations facilitating the transformation process. A small part is associated to the SMA creep (by reduction of hysteresis deformation span after the training part in the A–B–C–D sets of cycles). In addition, the Fig. 6 (left) indicates that at 0.01 Hz the temperature in the specimen can change by ±12 K during the transformation and in the retransformation compared with the mean room temperature. This global rough amplitude of 21 K produces a change of stress close to 132 MPa. This value is of the same order to the corresponding value in Fig. 3 and represents 2/3 of the hysteresis (1/3 in loading and 1/3 in unloading) width in the 100th cycle in Fig. 7 (left). The change in the first 100 slow cycles (see, Fig. 7 left) was from 15.82 to 5.05 J (diminishes 68%). In 400 cycles at 3 Hz the evolution of energy is from 1.8 to 1.2 J (diminishes 33%).

Studying the hysteresis energy against the cycling frequency shows that their value changes with cycling. Two main effects can be observed. The first is an intrinsic effect (dislocation creation, interaction between grain boundaries an so on) as shows the Fig. 7 (left). The second action is the effect of the temperature actions. Figure 8 shows the changes on hysteresis width against the cycling frequency. The change indicated by a–b dots in Fig. 8 (right) is associated to a supplementary intrinsic effect produced by the set of fast cycles (maximal deformation 8%). The position of the maximal value of hysteresis width is situated at 0.01 Hz for the 2.46 mm of diameter. For wires of

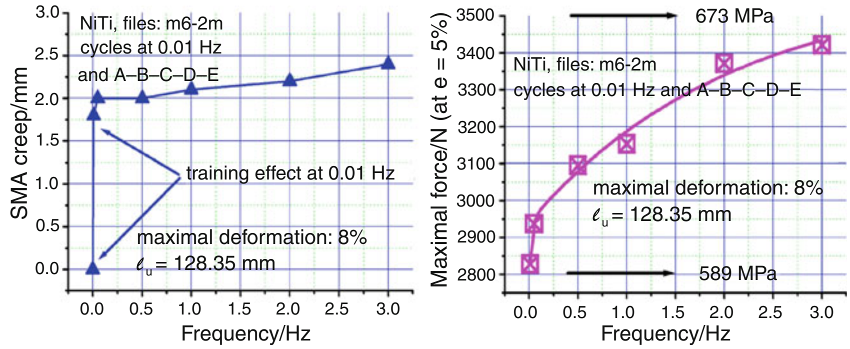

Fig. 9 Cycling effects for a maximal deformation of 8%. *Left*: SMA creep in NiTi SMA. After the training effect the supplementary creep increase do not overcomes 20%. *Right*: Force increase (20%) related with the temperature boost up at rising frequencies

lower diameter the heat transfer to surroundings is more effective and the maximum is situated at higher frequency.

The SMA creep effect after the training procedure for the A–B–C–D–E sets of cycles (see Fig. 6) is shown in Fig. 9 left. It can be observed that it is not highly relevant (1.8–2.4 mm or an increase of 0.5%) for the material studied. Thus, the pre-training (100 cycles at 0.01 Hz) is an effective method to nearly suppress the creep in further cyclings.

For higher deformation (8%) the progressive increase of mean temperature (more than 20 K at 3 Hz extracted from Fig. 6) produces an increase of stress (see, Fig. 9 right). Their value approaches 590 N or 125 MPa that, via Clausius–Clapeyron equation represents 20 K. The effect facilitates the increase of SMA creep and reducing the fracture-life. The increase of temperature is critical for the cycling life of the sample (see Fig. 10). A larger life is obtained for 200 MPa or lower stresses, corresponding for the samples used (2.46 mm of diameter) for forces near or under 1 kN. At this lower level the material life is highly sensitive to load. An increase of 250 N (50 MPa) or from 200 to 250 MPa reduces the mean number of working cycles from "2 to 4 millions of working cycles" to 100,000 cycles.

The fatigue-life for NiTi of 2.46 mm of diameter is represented in Fig. 10. The results include different

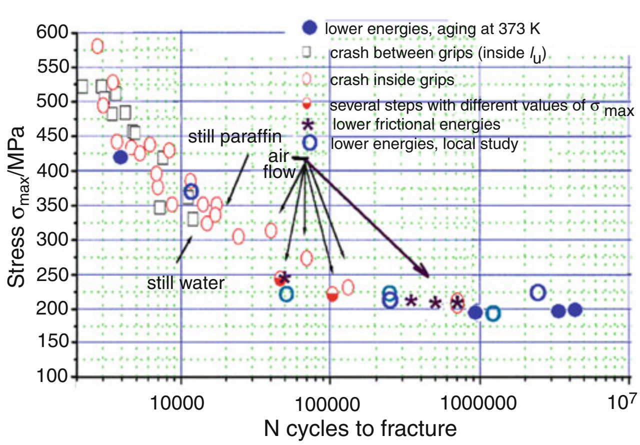

Fig. 10 Evolution of the fatigue-life for NiTi (2.46 mm of diameter) with the external stress for several sets of measurements

attempts to increase the life: use of local bath with still water or paraffin. The increase of life requires a reduction of stress in cycling that can be performed via short deformation cycles (i.e. less than 2%) and also, with the support of larger aging times at 373 K that reduces the critical stress of transformation by an increase of Ms. The fracture-life greatly increases for stresses less than 200 MPa.

When the application relates the stayed cables for bridges, the required number of cycles is extremely higher. For a storm of 3 or 4 days the expected number of working cycles can overcome 269,200 cycles (3*86,400) for the fundamental frequency (1 Hz) in the Iroise Bridge. One higher harmonic frequency is also present: 3 Hz or the same time requires increased fatigue-life. For instance, more than 800,000 cycles. The situation is clearly more demanding, for instance, in the St Nazaire Bridge. One of the basic frequencies is close to 18 Hz [L. Dieng, LCPC Nantes, private communication 2009].

Elementary heat transfer model using only one-body

The dissipation related to latent heat (W_l) and to hysteresis (W_h) in transformation-retransformation process when positive, increase the local temperature of the sample. The local temperature change in the heat capacity C is associated to (dT/dt). Also, a loss of power to the surroundings at temperature T_{amb} via a Newton cooling law by $P(T - T_{amb})$ is considered. The heat power balance equation (the one-body or the Tian equation) reads:

$$W_l + W_h = C\frac{dT}{dt} + P(T - T_{amb}) \quad (6)$$

Figure 11 outlines the power balance in the sample. The dissipated power (latent heat and work lost by hysteresis) is schematically represented in Fig. 12. The temperature T is calculated via an extremely elementary numeric approach using a FORTRAN program and the subroutine rk4 (a fourth-order Runge–Kutta) extracted from Numerical Recipes [10].

Two cases are considered in the simulated power input at 0.001 and 0.1 Hz. In Fig. 12, the simulated sinusoidal

Fig. 11 Power balance between dissipation inside the heat capacity *C*, the local increase of temperature (*T*(*t*)) and the heat-power send to surroundings by the coefficient *P*

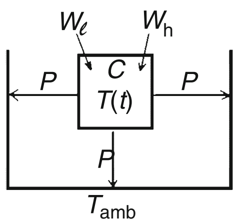

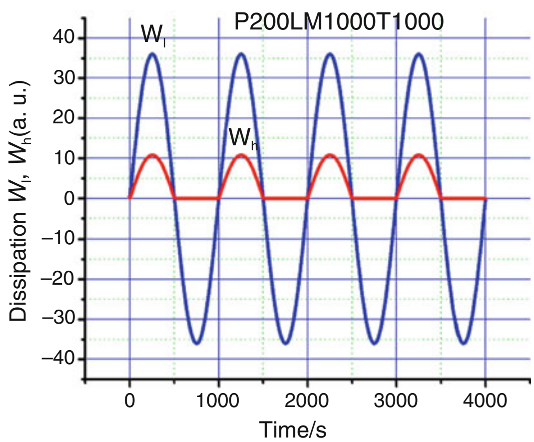

Fig. 12 *Larger signal*: simulation of latent heat (positive and negative as released and absorbed power W_l) by a sinusoidal signal. *Shorter signal*: simulation of one dissipation associated to hysteretic behavior (W_h). In the simulation the choice of cycling frequency is 0.001 Hz

shape of latent heat and the hysteresis heat. The hysteresis contribution is considered added to a latent heat contribution only in the transformation part.

The temperature in the simulated sample is visualized in Fig. 13 for the two frequencies studied (0.001 and 0.1 Hz). The simulated results show that at 0.001 Hz, the temperature tracks the external stress with a practical symmetrical evolution over and under the room temperature. In the computerized simulation Celsius scale (20 °C or 293 K) are used as shows Fig. 13. For 0.1 Hz the simulation shows one reduction of the temperature span plus one progressive evolution to and steady state with increased mean temperature. At lower frequencies the temperature tracks the

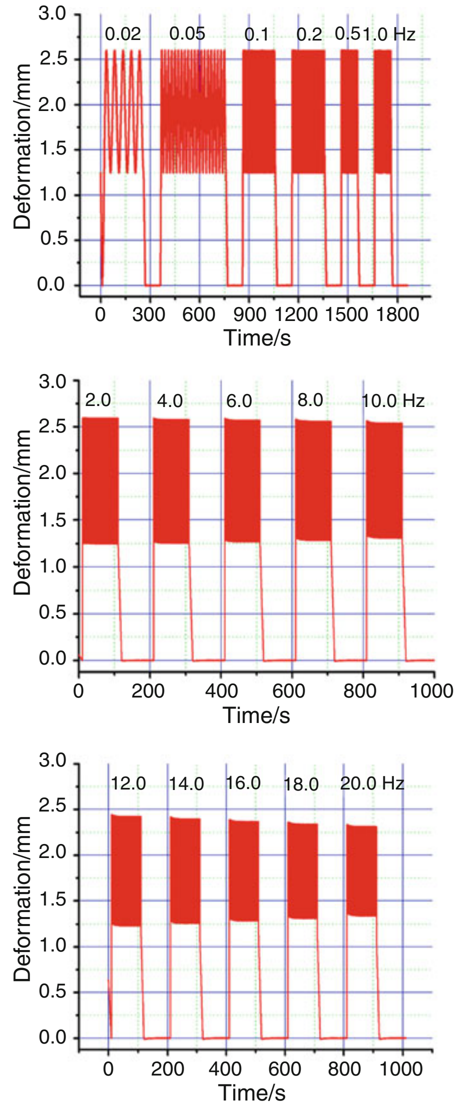

Fig. 14 Progressive reduction of the nominal deformation (established in 1.25% of the sample) induced by the artifact effects by the MTS equipment

transformation/retransformation by increase/decrease of the temperature around the "room temperature" at higher frequencies the temperature increase progressively to a

Fig. 13 Calculated temperature via the one heat capacity model and Runga–Kutta iterations starting at 20 °C. *Left*: slow cycles at 0.001 Hz. *Right*: "fast" cycles at 0.1 Hz

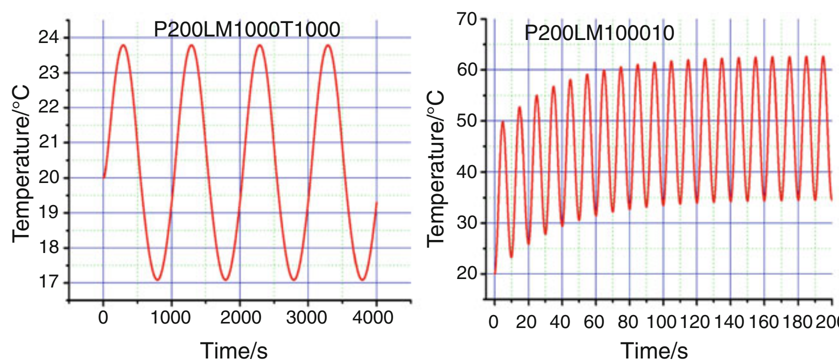

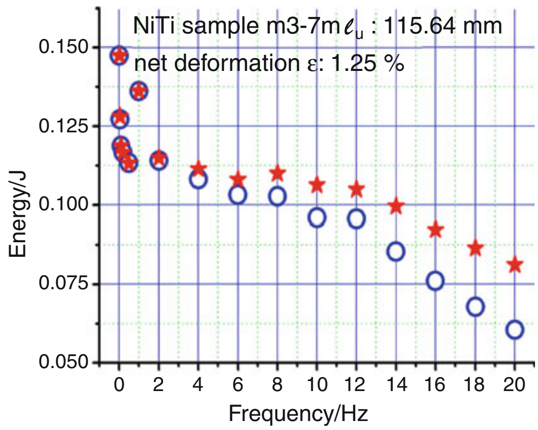

Fig. 15 Hysteresis energy values for lower deformation (1.25%) against the cycling frequency. *Open dots*: direct measurements of the hysteresis energy. *Starts*: energy values adapted by the ratio of the actual amplitude modified by the MTS equipment

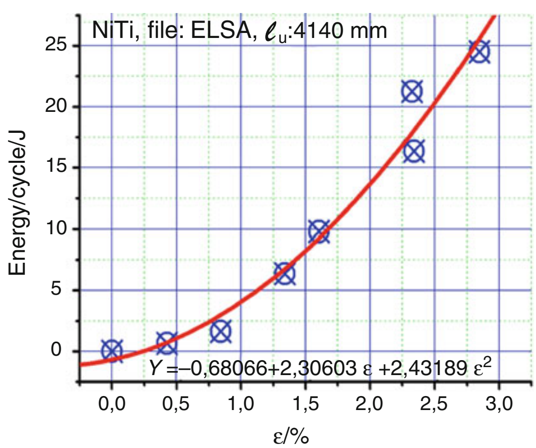

Fig. 16 Dissipated energy by the hysteretic cycles at lower deformation (ε) using a NiTi wire of 4.14 m. The experimental results are fitted by one quadratic form for lower cycling frequency (i.e., near 0.05 Hz) in stress–strain hysteretic measurements

steady state limit associate to transfer of hysteretic dissipation to surroundings.

Artifact effects in hysteretic analysis

When uses low deformation and higher frequencies the experimental conditions are relatively difficult to track for the hydraulic system that controls the MTS equipment. In fact, the equipment progressively reduces the span of predetermined deformation as shows the Fig. 14. The loss of relevancy starts for frequencies overcoming 2 Hz, the main effects start at 4 or 6 Hz and the amplitude is progressively reduced and, at 20 Hz, the value is diminished near 25%.

Figure 15 shows the direct evolution of the energy against the cycling frequency (open dots), the hydraulic equipment reduces the expected deformation and the hysteresis energy. Using one simple proportionality rule with the change of deformation created by the MTS the high relevant decrease of the energy is reduced (i.e., the full starts). The decrease of energy for frequencies overcoming 8–10 Hz is probably reduced that indicated in the figure. In fact, the cycling energy at lower deformations is not linear but is quadratic (as shows the Fig. 16) with the deformation length and the energy is more constant against the frequency that a simple proportional correction as indicates the stars in Fig. 15.

Figure 16 shows the energy when cycles are realized at lower frequency and lower deformation percent (under 3%). The experimental data fits via a polynomial approach of second degree. In Fig. 16, the used available length (l_u) overcomes 4 m (4.14 m) and the energy is calculated from experimental cycles done with this large length. The system relates one practical experiment used in damping of the cable 1 in the ELSA facility (Joint Research Center—EU, Ispra, Italy).

Conclusions

1) The temperature effects are highly relevant in the behavior of the SMA. At lower cycling frequency the temperature tracks the external stress and shows one oscillatory character with values under and over the room temperature. When the frequency increases, the dissipation effect of the hysteresis cycles increases their relative effect and the temperature increases to one steady state than can increase the plastic effects and reduces the life. In particular, these effects are highly relevant for the NiTi alloy.
2) For the NiTi, the particular behavior of the temperature in the sample can be roughly modeled via an elementary model using only one heat capacity or using a crude approach between the speed of transformation zone and the temperature shape (i.e., via a Gaussian propagation). The model is coherent with a change of behavior of temperature and transformation front from low cycling frequencies and relative fast cycling. At low frequencies the temperature affects the local transformation stress. At faster cycling the transformation front only remains in contact with the mean temperature of the sample and the stress is reduced. This effect is also relevant in the hysteresis width. With an increase of cycling frequency from 0.0001 to 3 Hz the hysteresis width is reduced to a quarter.

3) The analysis shows that the hysteresis width is mainly connected to temperature and, also to internal mechanisms induced by cycling that eventually, can reduce their width. The effect is more relevant in the first 100 cycles at 8% of deformation (the training part), the width is roughly reduced to a quarter.
4) The interest in highly fatigue-life and working at fast cycling (i.e., between 1 and 20 Hz) requires reduced transformation per cent (i.e., under 2%). At this level, the maximal mean temperature increase is reduced to 10 K. The measurements are affected by artifacts in the classical hydraulic equipment of stress–strain but the measurements and their analysis suggest that the dissipated energy seems practically constant to 20 Hz.

Acknowledgements Work realized in the frame of projects, SMARTeR (by European Science Foundation and MEC-MICINN) and "Smart materials and systems" (by M Fomento ref. 22/06) its economical support is gratefully acknowledged. V. T., acknowledges the MICINN for the grant PR2008-0235 that permitted the preparation of this work and to Pablo Riquelme (CAB) for their support in the MTS and INSTRON fatigue measurements. A.S. is thankfull for the support of Conicyt-Chile by the grant 1070370. The support from Bea Zapico and Daniel Tirelli in the study of low deformations in larger wires of NiTi SMA is gratefully acknowledged.

References

1. Torra V, Isalgue A, Martorell F, Terriault P, Lovey FC. Built in dampers for family homes via SMA: an ANSYS computation scheme based on mesoscopic and microscopic experimental analyses. Eng Struct. 2007;29:1889–902.
2. Torra V, Pelegrina JL, Isalgue A, Lovey FC. Metastable effects on martensitic transformation in SMA (I): recoverable effects by the action of thermodynamic forces in parent phase. J Therm Anal Calorim. 2005;81:131–5.
3. Sepulveda A, Muñoz R, Lovey FC, Auguet C, Isalgue A, Torra V. Metastable effects on martensitic transformation in SMA. Part II: the grain growth effects in Cu–Al–Be alloy. J Therm Anal Calorim. 2007;89(1):101–7.
4. Auguet C, Isalgue A, Lovey FC, Pelegrina JL, Ruiz S, Torra V. Metastable effects on martensitic transformation in SMA. Part III: tentative temperature effects in a NiTi alloy. J Therm Anal Calorim. 2007;89(2):537–42.
5. Auguet C, Isalgué A, Lovey FC, Martorell F, Torra V. Metastable effects on martensitic transformation in SMA. Part 4 thermomechanical properties of CuAlBe and NiTi observations for dampers in family houses. J Therm Anal Calorim. 2007;88(2): 537–48.
6. Carreras G, Isalgue A, Torra V, Lovey FC, Soul H. Metastable effects on martensitic transformation in SMA. Part V: fatigue-life and detailed hysteresis behavior in NiTi and Cu-based alloys. J Therm Anal Calorim. 2008;91(2):575–9.
7. Isalgue A, Torra V, Yawny A, Lovey FC. Metastable effects on martensitic transformation in SMA. Part VI: the Clausius–Clapeyron relationship. J Therm Anal Calorim. 2008;91(3):991–8.
8. Auguet C, Isalgue A, Torra V, Lovey FC, Pelegrina JL. Metastable effects on martensitic transformation in SMA. Part VII: aging problems in NiTi. J Therm Anal Calorim. 2008;92(1): 63–71.
9. Gibkes J, Bein BK, Pelzl J, Wieck A, Frenzel J, Eggeler G, et al. Processing induced change of thermal transport properties of NiTi-shape memory alloy. Acta Phys Pol A. 2008;114(6): A97–101.
10. Routine rk4 extracted from Numerical Recipes FORTRAN 77 version 2.07 Cambridge University Press UK included in the Microsoft Fortran PowerStation tool.